Spring 3-30-2023

Application of Direct Simulation Monte Carlo Method to Computation of RF Signal Degradation During Hypersonic Flight

Andrew DeRubertis
Washington University in St. Louis

WASHINGTON UNIVERSITY IN ST. LOUIS

McKelvey School of Engineering

Department of Mechanical Engineering and Materials Science

Thesis Examination Committee:

Ramesh K. Agarwal, Chair

Swami Karunamoorthy

David Peters

Application of Direct Simulation Monte Carlo Method to Computation of RF Signal Degradation During Hypersonic Flight

by

Andrew James DeRubertis

A thesis presented to

the McKelvey School of Engineering

of Washington University in

partial fulfillment of the

requirements for the degree

of Master of Science

May 2023

St. Louis, Missouri

Table of Contents

List of Figures

List of Tables

Acknowledgements

First of all, I would like to thank Dr. Agarwal for his constant support, knowledge, and encouragement throughout my time researching and innovating with him. Dr. Agarwal has taught me about aerodynamics and computational fluid dynamics, allowing me to find a passion that I plan to make a long career out of. I also want to thank Dr. Dave Peters and Dr. Swami Karunamoorthy for taking the time to be on my thesis committee, read my thesis, and listen to my presentation and defense. I also want to thank my classmates from our research lab group for their encouragement, for setting a positive example, and for driving me to want to innovate every day.

This thesis is dedicated to my family - Mom, Dad, Emily, Erin, and Liam. Your constant love, encouragement, humor, and support throughout my academic endeavors has helped me persevere through tough times and always believe in myself.

Andrew DeRubertis

Washington University in St. Louis

May 2023

ABSTRACT OF THE THESIS

Application of the Direct Simulation Monte Carlo Method

to Computation of RF Signal Degradation

During Hypersonic Flight

by

Andrew DeRubertis

Master of Science in Aerospace Engineering

Washington University in St. Louis, 2023

Professor Ramesh K. Agarwal, Chair

In order to further understand the hypersonic blackout problem, the first step is to investigate models to quantify signal degradation and begin implementing these models to representative plasma sheath and flow data. This research is the first attempt at implementing a model to predict RF signal degradation through the plasma sheath surrounding the hypersonic air vehicle. The investigation is performed using a Direct Simulation Monte Carlo (DSMC) based flow solver. The dsmcFoam solver in the OpenFoam library is used to simulate the flow around hypersonic bodies to obtain flow field properties, most importantly the electron number density profile, to aid in the calculations of signal degradation. The study of viability of RF communications from hypersonic, fixed-wing aircraft are paramount to the future of hypersonic military capabilities and even hypersonic travel. Predicting signal degradation for a transmission along a line of sight in real-time can eliminate radio blackout by guiding the gain models on the signal decoding side and allowing reconstruction of the transmission. Even without reconstruction, accurately predicting when signals will be unrecoverable can serve as an indicator for a hypersonic vehicle to send communications to a different ground station or satellite.

The integration method employed to integrate over the output electron number density profile yields values for attenuation that drop below 100 decibels in the transmission window of 10 to 30 GHz. Outside of this transmission window, attenuation and phase shift are high indicating poor chance of viable communication. If signal degradation models can be verified and improved with the flight data in the future, these results suggest that vital radar and satellite communications are possible through the plasma sheath and can be decoded using accurately predicted degradation values.

Chapter 1: Introduction

1.1 Motivation. As superpowers across the world race towards technological and engineering advancements that beget military supremacy, hypersonics has become an important area of research and development. Previously, hypersonics research focused on reentry aerodynamics and thermodynamics for blunt space capsules and the space shuttle. In the past decade, improvements in flow simulation algorithms, computing power, and the performance of high temperature materials have all contributed to rekindling of hypersonic activity, but this time with a different application in mind - the high speed, fixed-wing aircraft and high speed weapon systems. Hypersonic research projects such as NASA's X-43 series, Boeing and AFRL's X-51A, and Lockheed Martin and DARPA's HTV-2 programs are examples of the acceleration of hypersonic activity in recent years and emphasize the need for flight test data. Current issues the industry faces with hypersonics include the challenges of heat ablation and ablative materials' effects on the flow, ability of materials to face extreme surface temperatures and heat fluxes, and sustaining ramjet/scramjet propulsion. One additional issue in hypersonics, the issue that this thesis seeks to address, is the formation of the plasma sheath around a hypersonic aircraft and thereby the communication loss resulting from this phenomenon.

Intrinsic to the nature of plasmas are very strong electric and magnetic fields that interfere with signals transmitted from a hypersonic aircraft. Low frequency transmissions are unable to pierce this "shield" and even high frequency transmissions are often degraded beyond recoverability. While aerospace engineers have been fighting this problem since the inception of space travel, this problem became more known in the 1990's after the famous Hollywood film, Apollo 13. The radio blackout issue is portrayed in several scenes in the film.

Behind the scenes of space travel, engineers have considered many different solutions to the radio blackout problem. Some of these solution paths include changing transmission sensor locations and using magnetic materials along an aircraft near the sensors in order to create magnetic fields that combat the strong magnetic fields from the plasma. One solution path that has not yet been thoroughly investigated, is improving the quantification of signal degradation in the plasma sheath itself [1]. This thesis outlines the use of existing theoretical equations derived from the RF signal

propagation vector to calculate the attenuation and phase shift of different frequency signals sent from a hypersonic aircraft engulfed in a plasma sheath. DSMC flow simulation method is used in tandem with a quasi-trapezoidal, post-processing integration through the plasma sheath to obtain meaningful degradation values from the governing equations.

A critical plasma frequency can be found such that below this frequency all signals are completely destroyed [2]. RF signals above this critical plasma frequency are attenuated and undergo a phase shift, but theoretically they can pierce through the sheath and transmit to the receiver albeit arriving as degraded signals. Hypersonic test flight data is difficult and expensive to obtain and the majority of the data that does exist is classified. Wind tunnels are not a realistic option to simulate hypersonic aircraft surrounded by a plasma sheath because it is difficult to replicate the temperatures of this sheath. Due to the scarcity of data for verification, the main goal of this research is to pioneer the creation of a degradation calculation method and to show how to implement this method. Future work is necessary to incorporate magneto-hydrodynamic effects on the electron number density profile around the vehicle, but this model should serve as the basis for future high fidelity models. The effectiveness of this method can be extended by allowing quick adjustments to aircraft coordinates and altitude - they allow for optimization of receiver location based on the degradation calculated along different lines of sight from the aircraft.

Appendix A includes a brief description of additional research that was conducted in an independent study course with Dr. Agarwal. This work is the precursor to the main body of work in the thesis and thus was also conducted using the DSMC Method. The preliminary research uses a different solver method and seeks to analyze heat ablation effects in hypersonics.

1.2 Brief Review of Literature. A great deal of work has been done on investigating the effects of plasma on sensor performance from a hardware perspective, and significant work has been done into understanding electron density turbulent fluctuations in the hypersonic plasma layer. During his time at The University of Michigan, Iain Boyd, a prominent hypersonics researcher and professor at The University of Colorado, Boulder, and Lauren Mackey, a PhD student, focused on the effects of hypersonic plasma on sensor performance based on surface temperature of the sensor and its transmitted signals [2]. While no values for attenuation and phase shift are given, they have suggested

a simplified equation for calculating the attenuation. This equation simplifies the attenuation equation from another paper from Boyd's lab, however both equations depend upon the transmitted signal frequency [or wavelength], and the plasma frequency. Mackey and Boyd's paper concludes that high frequency RF signals would not be distorted at the flow conditions considered, however this thesis seeks to numerically investigate if that is true and if some degradation is present, can we implement a model to quantify it? Most importantly, it should be possible to adjust a model such that it can be used for lower altitude, higher Mach number, and higher Reynolds number flows where more degradation is present.

In a seminal paper published in Science Direct by two researchers from Northrup Grumman, T.C. Lin and L.K. Sproul took a more theoretical approach to derive the equations for attenuation and phase shift of RF signals through a plasma. This paper focused on the effects of electron number density turbulent fluctuations and the authors describe why it is very complex to quantify. Turbulent fluctuations in density and pressure in the plasma cause wave modulation of the electromagnetic wave fronts and these modulations cause fluctuations in the attenuation and phase shift of transmitted signals through the fluctuating plasma [3]. Because of the stochastic nature of DSMC particle sampling of plasma behavior, specifically collisions, and the representation of many real particles by one DSMC simulated particle, the turbulent fluctuating effects in the plasma are partially resolved because of the inherent spatial averaging nature of the solver. This is a simplification of real turbulent plasma behavior. However, because of the randomness of the fluctuations across the plasma, it should be sufficient for modeling the plasma behavior. This is also an area where additional research needs to be conducted in the future, with turbulent fluctuations being resolved on a refined scale and the line of sight integration incorporating a model for turbulent fluctuations from point to point along the line of sight.

1.3 Scope of Thesis. The scope of this thesis includes three areas of analysis as follows:

(1) Investigate on plasma behavior in the hypersonic plasma sheath surrounding a hypersonic vehicle
(2) Rigorous understanding and analysis of the DSMC method and its advantages for high-speed, quasi-rarefied and rarefied flows

(3) Developing a base model to quantify RF signal degradation through the hypersonic plasma sheath by calculating values for attenuation and phase shift

1.4 Publications and Previous Work During the M.S. Research. Table 1 lists the conferences where this research has been presented, as well as the papers and publications that have preceded this thesis. Some excerpts from these previous papers have been included in this thesis - they are clearly denoted in this thesis where material from previous papers was used.

Table 1 Publications and Previous Work by the Author

Name of Conference	Type of Paper	Dates
AIAA SciTech Forum, National Harbor, MD	AIAA Paper 2023-1609	January 24-26, 2023
32nd International Symposium on Rarefied Gas Dynamics (RGD), Seoul, South Korea	Conference Paper and AIP Publication (in progress)	July 4-8, 2022
Missouri Space Grant Consortium	Conference Paper	April 22-23, 2022

Chapter 2: Flow Solver Methodology

2.1 DSMC.

2.1.1 History of DSMC Method and Classical Use. The DSMC Method was developed by Graeme Bird, a professor at the University of Sydney, and is described in detail in his seminal book, **The DSMC Method** [4]. Initially, the method was primarily used for reentry aerodynamics, and considering that it was designed to analyze rarefied flows, this was the only feasible application of the method. However, more recent advancement in hypersonic capabilities has extended the importance of the DSMC method to high-speed, high-altitude weapon systems and hypersonic demonstration vehicles mentioned in the introduction. The DSMC method solves the Boltzmann equation, an equation that governs the fluid flow from continuum to rarefied regime. The Boltzmann equations applies to the continuum regime, as do the Euler and Navier Stokes equations, and all the way to free-molecular flow. Navier Stokes equations break down for non-continuum rarefied flows, since they represent a continuum mechanics model. To quantify when the Navier Stokes equations break down and a Boltzmann method should be employed, the Knudsen number is employed. The Knudsen number is defined as the ratio of the mean free path in a flow to a characteristic length scale, L_{char}.

$$Kn = \frac{\lambda}{L_{char}} \tag{1}$$

The criteria based on Equation 1 is qualitative. In continuum-transition regime if the Knudsen number is close to or larger than 0.1, then the flow can be considered as rarefied and a Boltzmann equation based method should be employed.

2.1.2 Current Applications of DSMC. One of the more recent applications the DSMC method is for simulation of flow over low earth orbit satellites or spacecraft. As previously mentioned, advances in high-speed, high-altitude weapon systems and recently developed hypersonic test vehicles have opened up a new area for application of the DSMC method.

2.2 DSMC Internal Models and Methods. Embedded within the DSMC framework are a number of internal models controlling which collisions occur, how they occur, and what effects these collisions have on the particles. It is important to note that different DSMC codes allow for different internal models to be implemented, and the current research is still evolving toward optimizing the accuracy of these models for different applications. In this thesis, the models available in dsmcFoam are employed. The first model is the variable hard sphere model that governs the path of particles after a collision. The second model is the 'No Time Counter' collision frequency model. This model was created by Graeme Bird. The 'No Time Counter' (NTC) method randomly selects pairs of particles from a computational cell and randomly selects a number between 0 and 1 [4]. A probability of a collision between the two particles is calculated and if greater than the randomly selected number, the collision is executed, otherwise the next collision pair is sampled and investigated [4]. Based on the number of particles in each cell, the method starts with an expected number of collisions for the time step, n_{coll}. Once n_{coll} collision pairs have been sampled, and a new number of collisions have taken place based on the results of the random sampling, the collision frequency for a time step is updated.

Another internal model used in the DSMC solver is the Larsen-Borgnakke internal energy model. This model governs the resulting internal energy of two particles after a collision occurs and how these particles exchange energy between translational energy and internal energy modes. For inelastic collisions, the Larsen-Borgnakke model samples the equilibrium distribution of internal and translational energies and assigns these values to the particles after an inelastic collision [5].

Lastly, an internal model is needed for gas surface interactions and the resulting reflection direction when a particle collides with the aircraft surface. Possible models are the specular, diffuse, and maxwell models. In the dsmcFoam a MaxwellianThermal model is used. This model samples the Maxwell-Boltzmann particle velocity distribution for a set temperature. This distribution is derived from the kinetic theory of gases, and is a Chi Square distribution scale with the Temperature and mass of a particle [6].

2.3 Advantages of DSMC. In addition to being crucially important to accurately modeling the rarefied, non-continuum flow, the DSMC Method also has computational advantages over deterministic methods. Because of the stochastic nature of the DSMC method, with its random

sampling of collision pairs, the mesh does not have to be as refined as with, for example, a RANS model which needs to resolve turbulent fluctuations on very fine spatial scales. Additionally, the representation of many (10e+9) real particles with a single simulation particle, reduces the computational cost of DSMC solvers.

Chapter 3: Simulation Methodology

3.1 Software and Hardware. The software used in this research is the dsmcFoam, a DSMC solver available in the open-source CFD library known as openFoam. All simulations were run serially on a Dell T3600 with 4 cores.

3.2 Boundary Conditions. The boundary conditions used in the simulations are an upstream velocity inlet condition and a downstream pressure outlet condition. The different inlet velocities correspond to Mach numbers of 5, 7.5, and 10 at an altitude of 95000 ft and the corresponding free stream properties at this altitude.

3.3 Geometries. The hypersonic bodies simulated in this thesis include an elliptic nose cone body with a length of 0.5 m and height of 0.2 m and a wedge, with a length of 0.5 m and a rear height of 0.2 m. These geometries are representative of the leading edge/nose of hypersonic missiles, drones, or space planes.

3.4 Mesh. Since the DSMC method employs the stochastic process of sampling a distribution of simulated particles in each cell, the mesh does not need to be as refined as the mesh required for a typical continuum solver based on the Navier-Stokes equations. However, there is a condition that must be met to ensure that the probabilistic model is valid for real collisions. Each cell's width and height, dx and dy must be smaller than one third of the mean free path [7]. The relation follows:

$$dx, dy < \frac{\lambda}{3} \tag{2}$$

The mean free path, λ, is the average distance a particle travels before a collision. It changes with altitude since the atmospheric density changes. At 95000 ft, the altitude of the simulation at which the flow boundary conditions are defined, the mean free path is about 1.5 mm [8]. Therefore, the largest mesh cells do not have a width or height greater than 0.5 mm. This discretization requirement ensures that within a cell, a collision will occur due the flow over the hypersonic aircraft, and not a random collision that takes place by particle movement over the mean free path. If the spatial discretization

was too large with respect to the mean free path, then the method would be sampling for random

collisions at the ambient conditions. Choosing a maximum width or height of one third of the mean free path solves this potential problem. The meshes used for the ellipse and the wedge are shown in Figure 1.

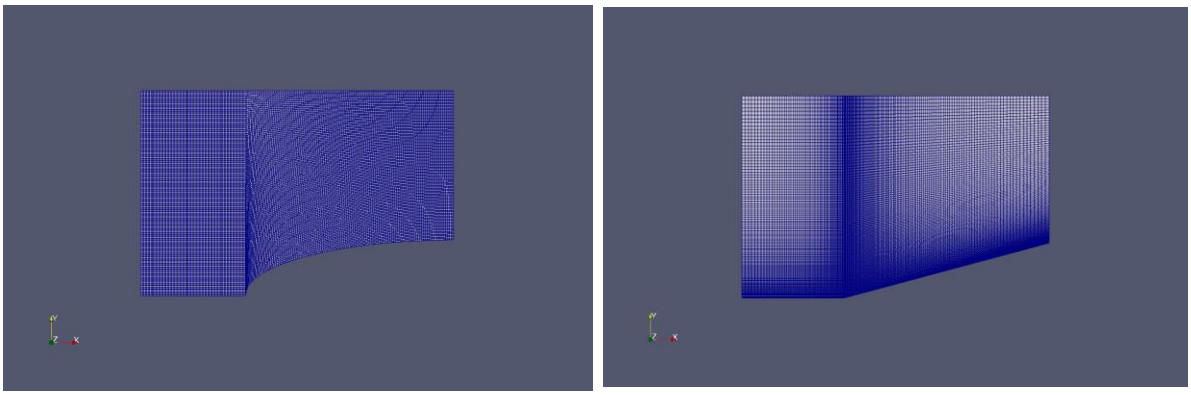

Figure 1 Meshes for an ellipse and a wedge.

Chapter 4: Post Processing Methodology

In the post-processing step, the line of sight integration through the plasma sheath is performed in MATLAB. With the non-uniform cell size used in the mesh, the difficulty in the post-processing step is to find the data points in the cells that are closest to the line of sight (LOS). Once these points that lay along the line of sight are obtained by a function minimizing the Euclidean distance from the LOS, the electron number density at these points and the distance between these points is used in a quasi-trapezoidal integration step. In MATLAB, the code allows for the user to either choose points in the domain that define the line of sight or input latitude and longitude coordinates with the altitude being fixed at 95,000 ft. to automate the line of sight choice. The boundary conditions and ambient flow conditions would change in the CFD solver step for changing altitudes.

In Figure 2, the plot on the upper left corner shows the data points that are read into the file along the line of sight. The 'minGridDist' plot in the upper right corner shows the points that are within some user-defined threshold distance from the line of sight. The 'LOS Points' plot in the lower left corner of Figure 2 shows the 15 closest data-points to the line of sight by Euclidean distance. Choosing 15 points was arbitrary, but seemed to capture the best results and any fluctuations in less dense regions of the mesh.

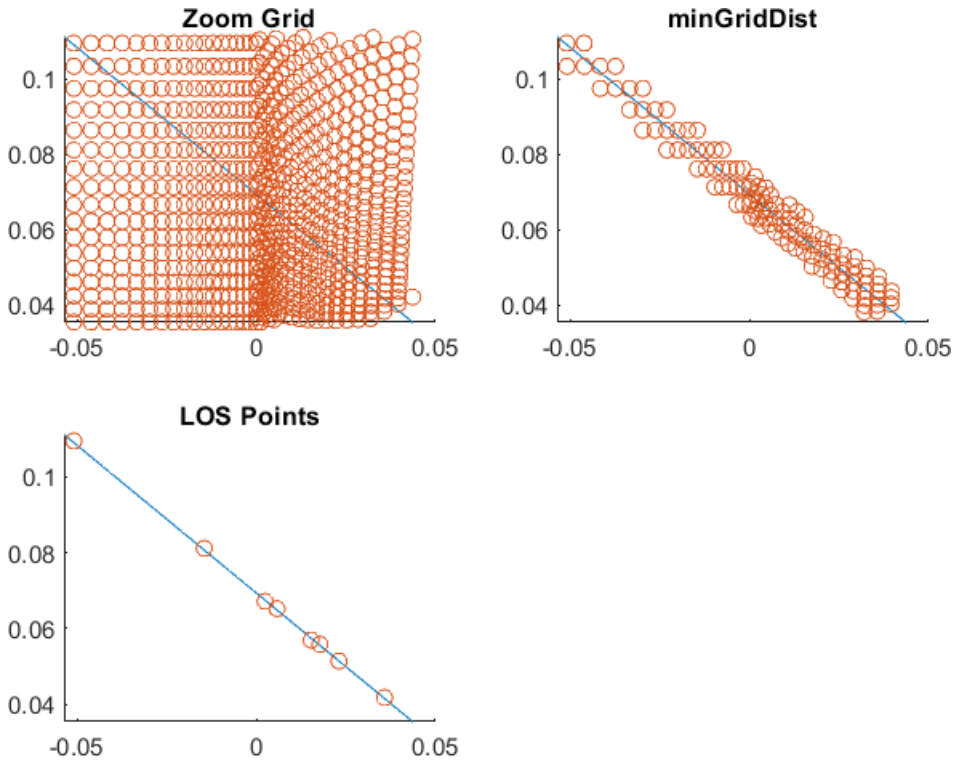

Figure 2 Selection Process of data points closest to Line of Sight (LOS)

The Lin Model is used which is derived from the EM wave propagation constant [3]. It follows

$$T = \int_a^b \alpha ds \tag{3}$$

$$B = \int_a^b \beta ds \tag{4}$$

The variable s represents the path through the plasma. The trapezoidal method is developed and used to solve Equations 3 and 4. The attenuation constant, α, and phase shift constant, β, can be expressed as:

$$\alpha = \sqrt{1 - \left(\frac{\frac{\omega_p}{\omega}}{1+\left(\frac{\upsilon_e}{\omega}\right)^2}\right)^2 + \left(\frac{\omega_p}{\omega}\right)^2 * \left(\frac{\upsilon_e}{\omega}\right)/\left(1 + \left(\frac{\upsilon_e}{\omega}\right)^2\right)^2 - \left[\left(1 - \left(\frac{\omega_p}{\omega}\right)^2\right)/\left(1 + \left(\frac{\upsilon_e}{\omega}\right)^2\right)\right]} \tag{5}$$

$$\beta = \sqrt{1 - \left(\frac{\frac{\omega_p}{\omega}}{1+\left(\frac{\upsilon_e}{\omega}\right)^2}\right)^2 + \left(\frac{\omega_p}{\omega}\right)^2 * \left(\frac{\upsilon_e}{\omega}\right)/\left(1 + \left(\frac{\upsilon_e}{\omega}\right)^2\right)^2 - \left[\left(1 - \left(\frac{\omega_p}{\omega}\right)^2\right)/\left(1 + \left(\frac{\upsilon_e}{\omega}\right)^2\right)\right]} \tag{6}$$

4.1 Parametric Study. In order to quantify signal degradation for a realistic situation with changing aircraft positioning and transmission frequencies, various angles of attack and Mach numbers were studied. A transmission frequency of 10 GHz is chosen since it is in the typical transmission range for large amounts of radar and communications data with satellites. Note that the transmission frequency could easily be changed within the model to calculate degradation for other frequencies. However, if the frequency of the signal is much lower than the critical plasma frequency, the signal will be too degraded to recover, therefore a relatively high transmission frequency is necessary for signal recovery to be possible [2]. Additionally, transmission from different chord-wise sensor locations is studied to understand how the plasma effects change from the leading edge moving aft along the aircraft.

The different angles of attack studied are -8, -4, 0, 4, 8, 12 and the Mach numbers are 5, 7.5, and 10. The sensor location is also studied. This is done in the post-processing step, when defining the line of sight and where it initiates along the surface of the vehicle. The sensor locations are placed at chord-wise locations that range from 10% of the chord to 90% of the chord.

Chapter 5: CFD Results

5.1 Study of Effect of Mach Number.

5.1.1 Ellipse at Mach 5. Pressure, velocity, and electron number density profiles around the ellipse at Mach 5 and zero angle of attack are shown in Figure 3, respectively. Similary, Figure 4 shows the same profiles from left to right around the wedge. All pressure values are in the figures are in kPa, velocity values are in km/s, and electron number density values in $\frac{\#}{m3}$ The pressure and velocity contours illustrate the oblique shock in front of the wedge and the detached shock in front of the ellipse, as expected. The peak electron number density around the ellipse at this flight condition is $9.6e + 20$, while the peak electron number density around the wedge is $3.5e + 20$.

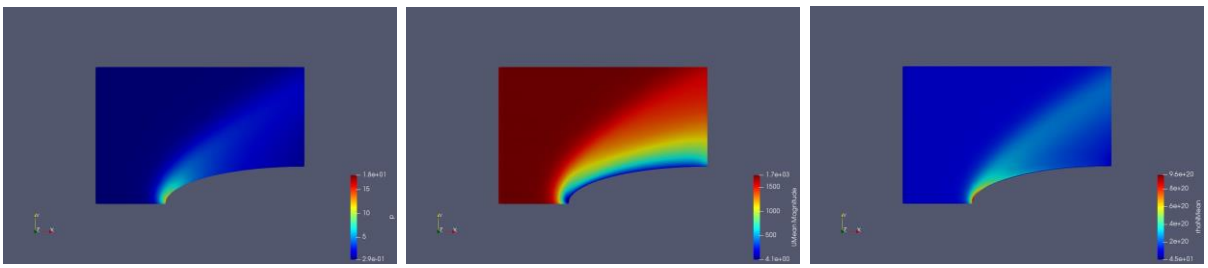

Figure 3 Pressure, velocity, and electron number density profiles around ellipse at Mach 5 and 0 degree angle of attack

5.1.2 Wedge at Mach 5. The peak electron number density around the wedge is $3.5e + 20$.

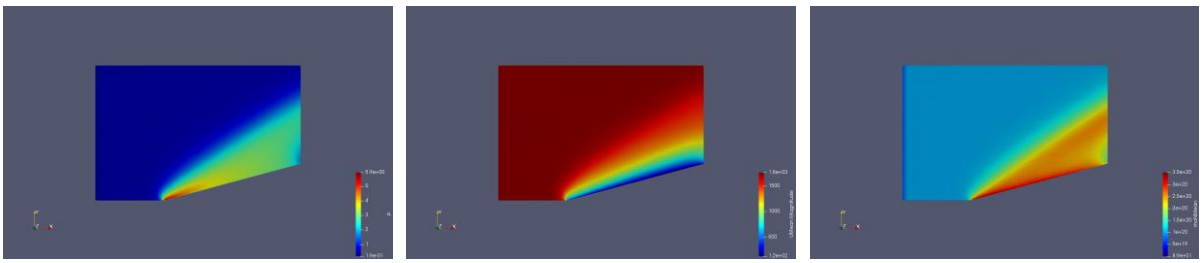

Figure 4 Pressure, velocity, and electron number density profiles around wedge at Mach 5 and 0 angle of attack

5.1.3 Ellipse at Mach 7.5. Pressure, velocity, and electron number density profiles around the ellipse at Mach 7.5 and zero degree angle of attack are shown in Fig. 5, respectively. Compared to the

Mach 5 case at zero angle of attack, the detached shock can be seen to be slightly closer to the surface of the ellipse, consistent with theta-Beta-Mach theory with increasing Mach number. Since the strong fluctuations in velocity and temperature across the shock lead to ionization, this is approximately where the plasma begins to appear. Therefore, as the Mach number increases, the plasma thickness slightly decreases. However, the peak electron number density around the ellipse increases slightly to $1.5e + 21$.

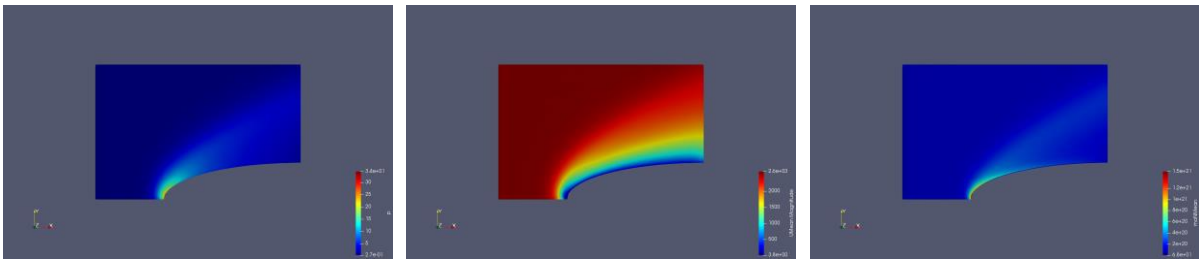

Figure 5 Pressure, velocity, and electron number density profiles around ellipse at Mach 7.5 and 0 degree angle of attack

5.1.4 Wedge at Mach 7.5. The wedge shows similar trends as in Figure 5, with the increasing Mach number leading to a thinner plasma layer, but with an increase in the peak electron number density. A thinner plasma is beneficial for signal transmission; however the increased electron number density can be detrimental. The peak electron number density around the wedge is now $4.7e + 20$. This increase of 34% in peak electron number density is less drastic than the increase around the ellipse of 56%.

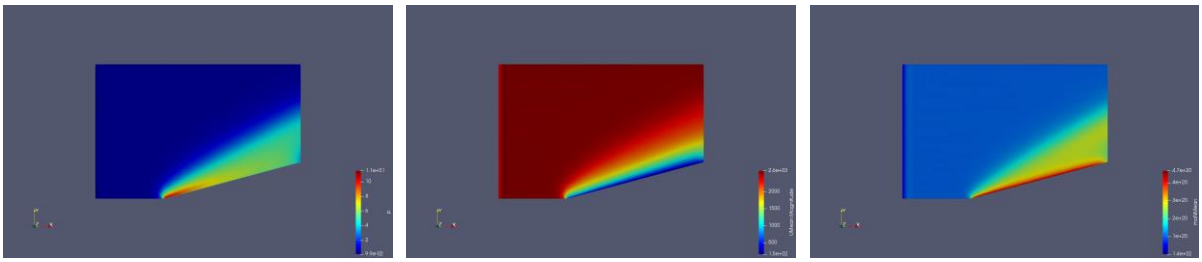

Figure 6 Pressure, velocity, and electron number density profiles around wedge at Mach 7.5 and 0 degree angle of attack

5.1.5 Ellipse at Mach 10. Figure 7 shows the same profiles around the ellipse at Mach 10 and

zero degree angle of attack. Once again, similar trends are seen with the thinner plasma layer, but

the peak electron number density increases to $2.0e + 21$.

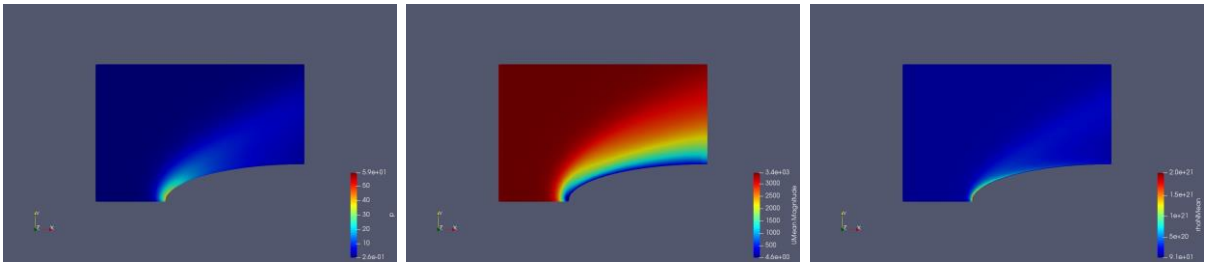

Figure 7 Pressure, velocity, and electron number density profiles around ellipse at Mach 10 and 0 degree angle of attack

5.2 Angle of Attack Study. The angle of attack study around the ellipse at Mach 5 are shown in Figures 8, 9, and 10. These figures show the pressure, velocity, and electron number density profiles at various angles of attack, respectively. In the figures, results start at the top left and end at the bottom right. The angles of attack are $\alpha = -8, -4, 0, 4, 8, 12$ from left to right. The same angle of attack sweep was studied around the wedge and similar profiles can be seen in Figures 11, 12, and 13 for the case of the wedge.

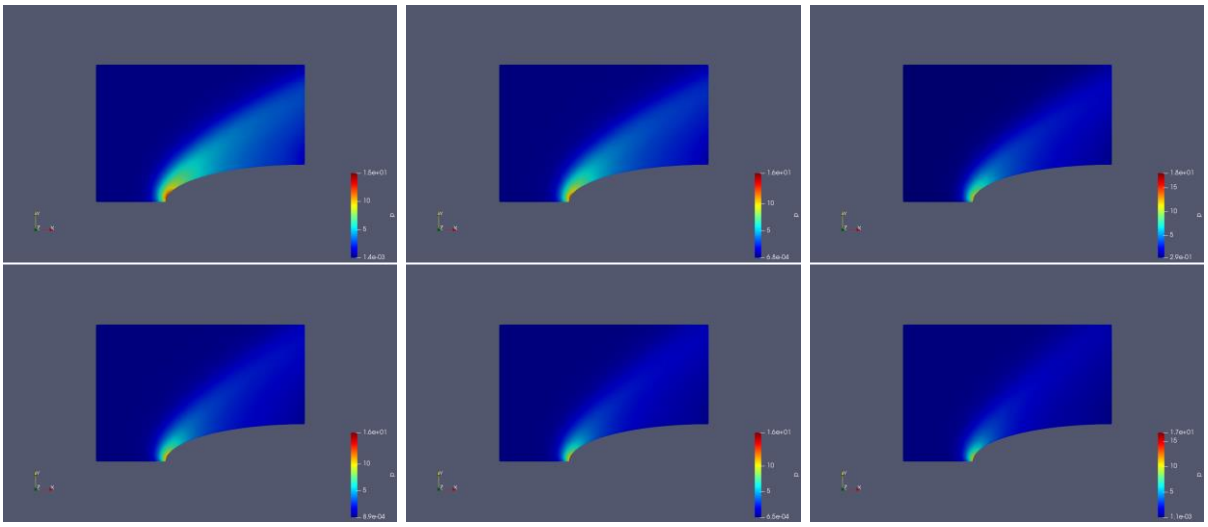

Figure 8 Pressure profiles around ellipse at Mach 5 and angles of attack -8, -4, 0, 4, 8, 12

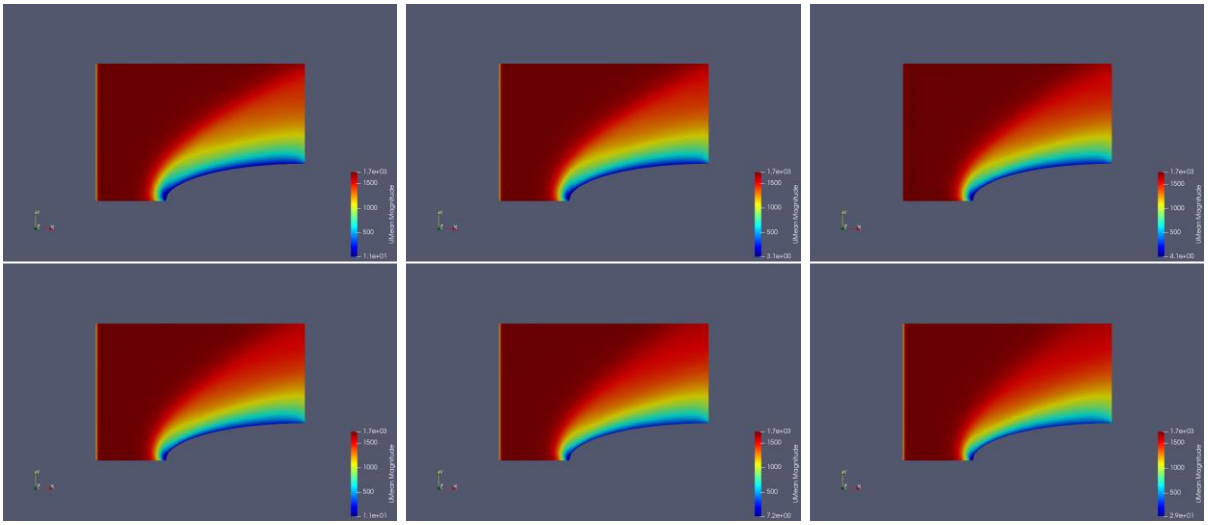

Figure 9 Velocity profiles around ellipse at Mach 5 and angles of attack -8, -4, 0, 4, 8, 12

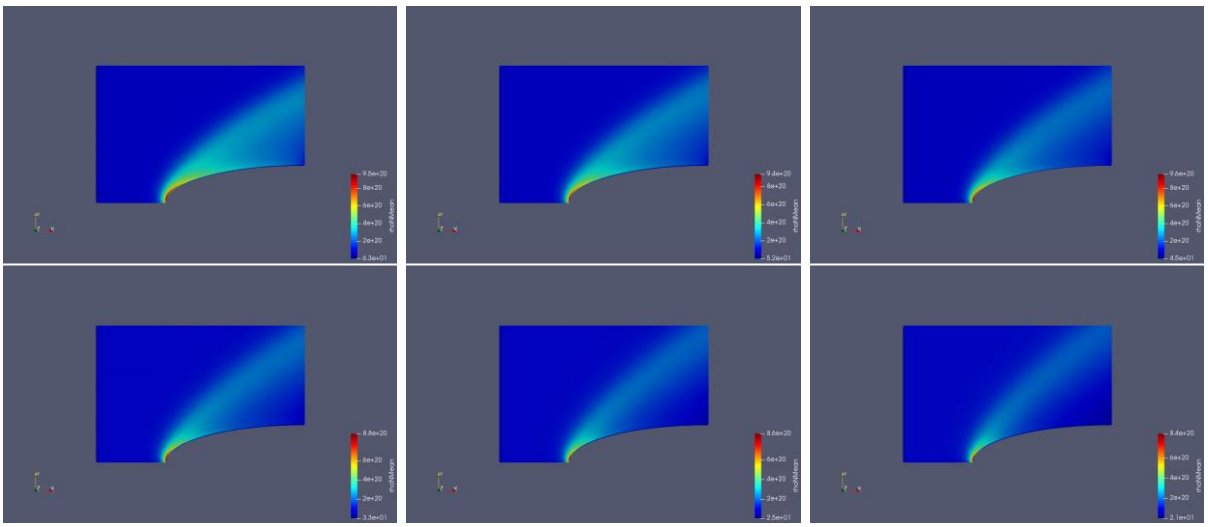

Figure 10 Electron number density profiles around ellipse at Mach 5 and angles of attack -8, -4, 0, 4, 8, 12

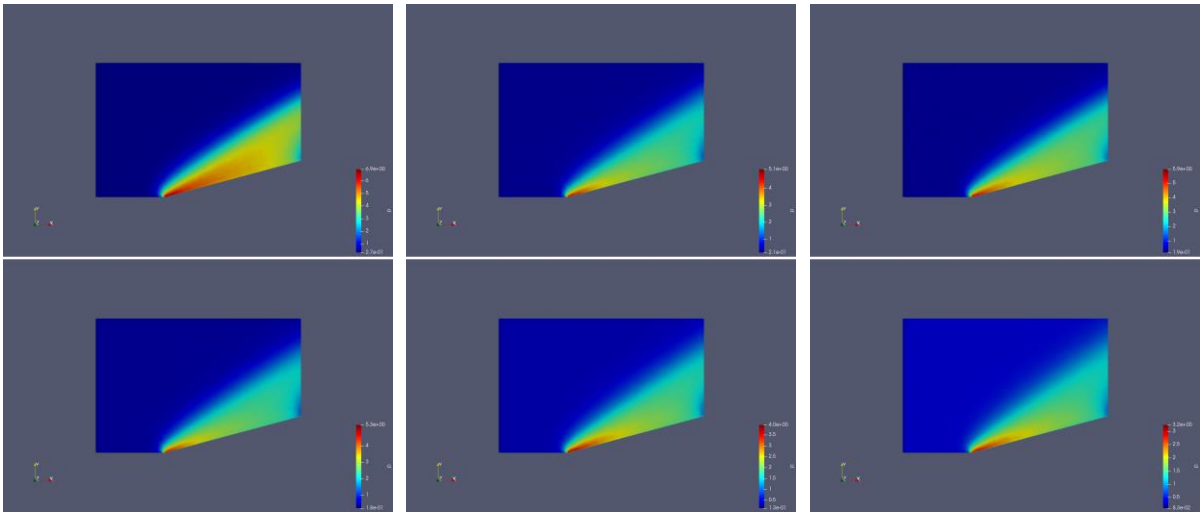

Figure 11 Pressure profiles around wedge at Mach 5 and angles of attack -8, -4, 0, 4, 8, 12

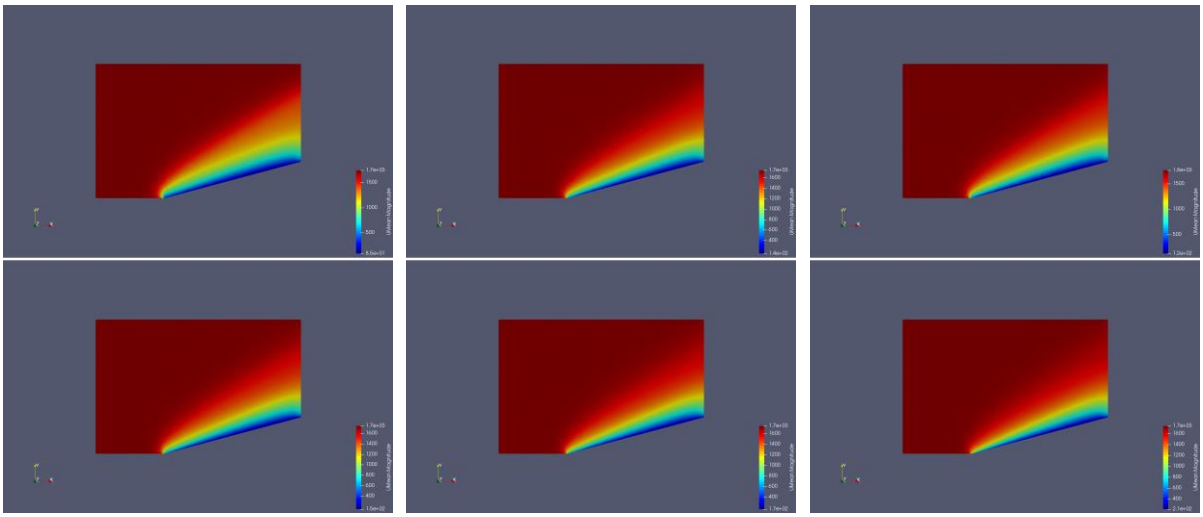

Figure 12 Velocity profiles around wedge at Mach 5 and angles of attack -8, -4, 0, 4, 8, 12

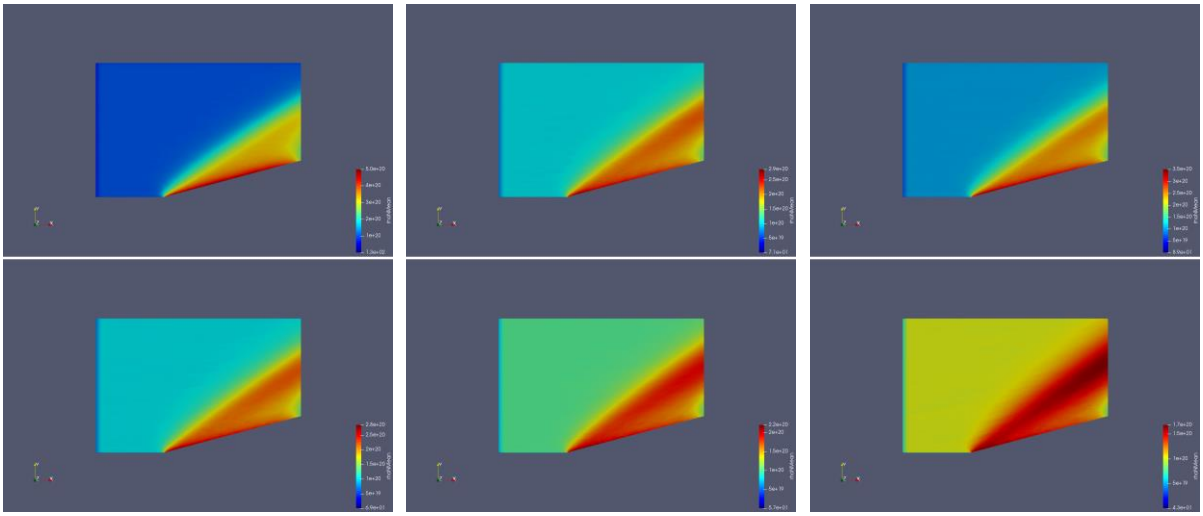

Figure 13 Electron number density profiles around ellipse at Mach 5 and angles of attack -8, -4, 0, 4, 8, 12

The angle of attack study around the ellipse shows that at lower angles of attack, especially at negative angles of attack, the pressure on the upper surface increases. Likewise, the electron number density grows. The plasma layer is thicker at these lower angles of attack, and the peak electron number density is higher, although only slightly. Both of these trends will lead to more degraded signals. The wedge shows similar trends, however the plasma thickness changes very slightly. The peak electron number density in the plasma along the upper surface increases at lower angles of attack and negative angles of attack. For both the ellipse and the wedge, higher angles of attack shield the upper surface and lead to a thinner plasma and lower peak electron number density, making this more ideal for signal transmission. The effects on the upper surface would be reversed on the lower surface, therefore actionable aircraft maneuvers would depend on whether the signal is being transmitted down to a receiver on Earth or up to a receiver on a satellite.

Chapter 6: RF Degradation Results

6.1 Angle of Attack Study. The angle of attack studies at Mach 5, 7.5, and 10 are performed for a sensor location at 40% of the chord and a line of sight assuming the signal is transmitted vertically from the surface. The transmission LOS can be adjusted in the model, but the same orientation of the transmission is needed to standardize the results for comparison.

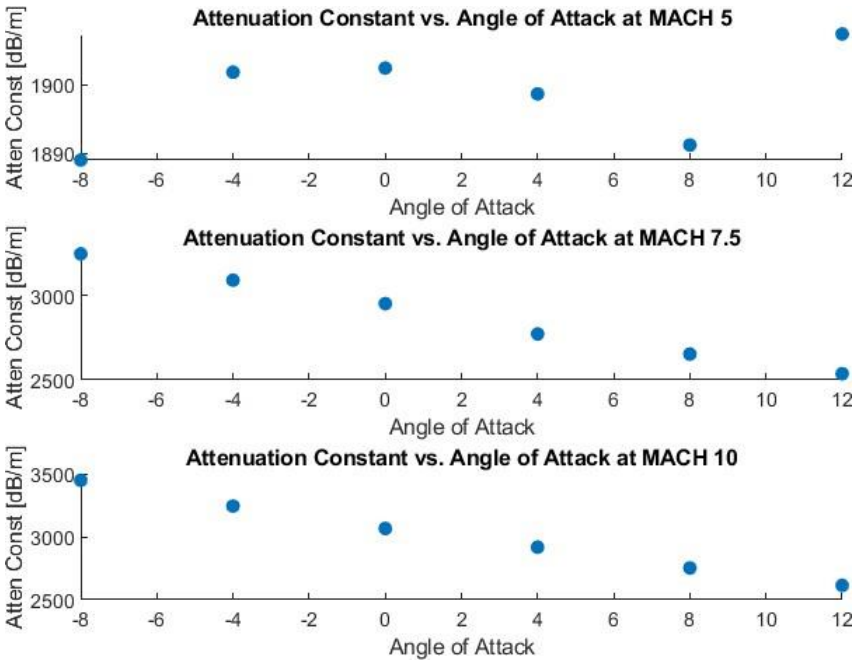

Figure 14 Angle of Attack Study for Ellipse - Attenuation vs. Angle of Attack

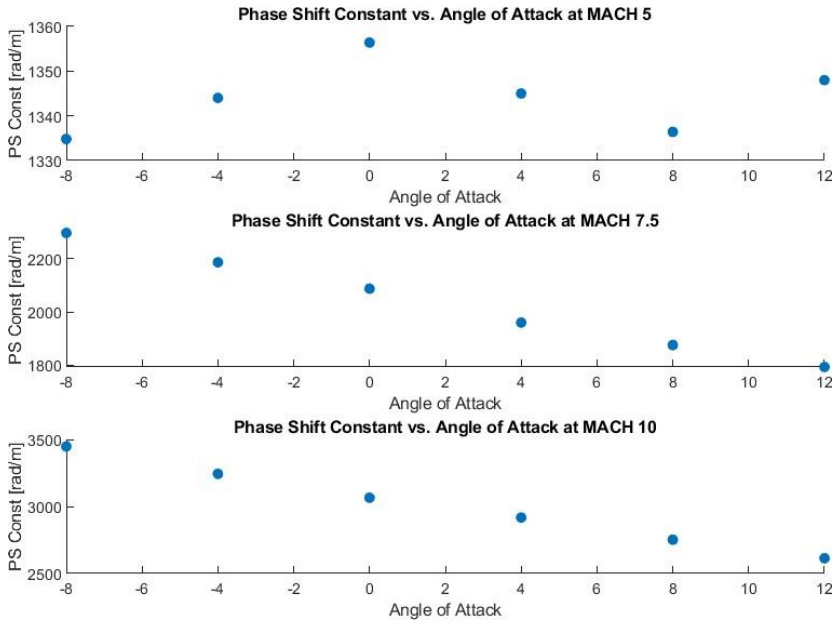

Figure 15 Angle of Attack Study for Ellipse - Phase Shift vs. Angle of Attack

Figure 14 and 15 show that at Mach 7.5 and Mach 10 the signal degradation is highest at negative angles of attack and lower positive angles of attack. The optimal angle of attack for transmission from the 40% of chord location is 12 degree. At Mach 5, however, there are some more interesting results. The minimum attenuation occurs at -8 and 8 degrees angles of attack, and the minimum phase shift occurs at the same angles of attack. This occurs because at an angle of attack of -8 degrees and at Mach 5, the flow is slow enough that the plasma is closer to the body surface and is thinner without the flow heating the plasma excessively and causing a high electron number density. On the other hand, at an angle of attack of 8 degrees the opposite occurs; the plasma is thick but the heating is not excessive and therefore the electron number density does not remain as high. At higher Mach numbers, these same trends are not seen because hotter temperatures change the rate at which ionization occurs. The plasma thickness effect dominates over the peak electron number density effect at higher Mach numbers, since electron number densities are still high enough to significantly degrade the signal.

6.2 Sensor Location Study at Mach 5. Figure 16 shows the results of the sensor location

study at Mach 5 and 0 degree angle of attack. The upper two plots in the figure show the attenuation

and phase shift per unit length, while the lower two plots show the attenuation and phase shift multiplied by the length of the plasma along the line of sight. The units are in decibels (dB) and radians, respectively. All sensor location study results are at zero angle of attack. Additionally, to standardize the results for comparison, the sensor location studies assume a vertical line of sight transmission. The line of sight will not always be vertical and this can be adjusted in the model, but it needs to be standardized to better understand how the plasma changes as the sensor moves aft.

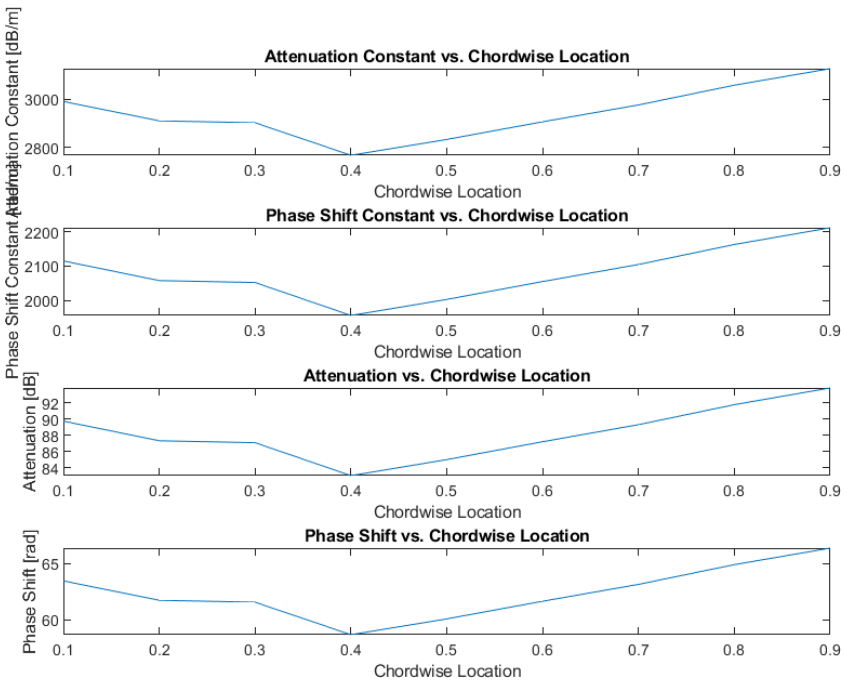

Figure 16 Sensor Location Study for Ellipse at Mach 5

For this case the attenuation and phase shift are both lowest for a sensor location around 40% of the chord. Forward to this location, the electron number density is higher, and aft of this location the plasma is thicker. At 40% of the chord, the plasma thickness is approximately 30 mm and the attenuation drops to about 81 dB and the phase shift to 58 rads.

6.3 Sensor Location Study at Mach 7.5. Figure 17 shows the sensor location study for the ellipse at Mach 7.5 at 0 degree angle of attack.

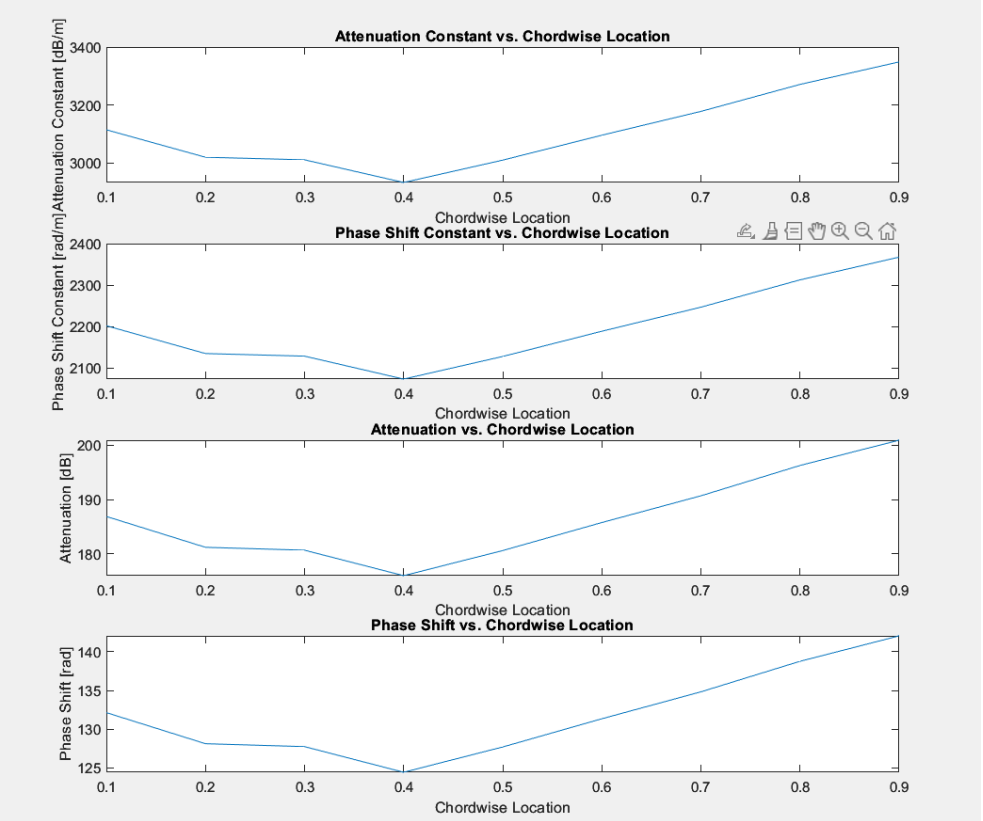

Figure 17 Sensor Location Study for Ellipse at Mach 7.5

The Mach 7.5 case shows trends similar to the Mach 5 case with the optimal sensor location at 40% of the chord. However, the sensor locations forward of 40% chord location perform better than at Mach 5. Forward of 40% of the chord the electron number density is higher, but the plasma is not as thick and as the Mach number increases the thickness decreases. Aft of 40% of chord the plasma is thick and the peak electron number density is higher than that in the Mach 5 case, so these locations are not ideal. This further illustrates the delicate balance between the electron number density and the plasma thickness. At 40% of chord the attenuation is about 88 dB and the phase shift is 61 rads.

6.4 Sensor Location Study at Mach 10. Figure 18 shows the sensor location study for the ellipse at Mach 10 at 0 degree angle of attack.

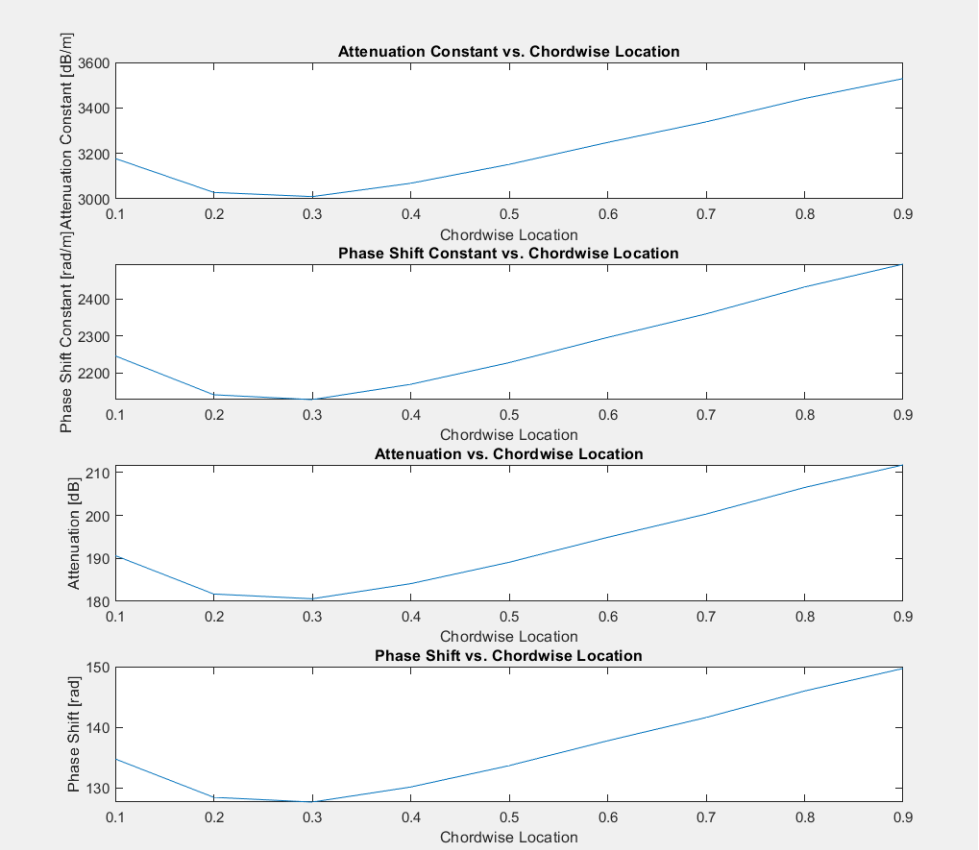

Figure 18 Sensor Location Study for Ellipse at Mach 10

At Mach 10, the optimal sensor location shifts to between 20% and 30% of the chord. Aft of this, signals are significantly attenuated. Near 20% and 30% of the chord, the attenuation is 90 dB and the phase shift is 64 rads.

Chapter 7: Conclusion

The research in this thesis can serve as a successful first step towards integrating a DSMC flow solver and post-processing of the simulation results with RF degradation models to predict signal degradation through the hypersonic plasma sheath. The decreased attenuation and phase shift in the SHF RF band suggest that vital radar and satellite communications may be possible through the plasma during hypersonic flight. In the study, effects of sensor degradation and heat ablation on the signal transmission are ignored, but can be introduced and overlapped in the future work. With improved parallel processing tools, the next step in this research may include utilizing parallel processing capability to solve electrons as kinetic particles instead of assuming quasi-neutrality of kinetic ions, an inherent assumption in the DSMC solver. Other well-known CFD software like NASA's DAC software also implement the DSMC method for hypersonic flow; the simulation models in this software can be compared in future work to establish a firmer idea of the model's fidelity even without test flight data. NASA's DAC software also introduces adaptive meshing to the DSMC solver, which is an important next step in all turbulent flows enhancing mesh refinement near large pressure gradients. Finally, availability of wind tunnel data and more importantly the test flight data to compare the results obtained with simulations would make this research industry-ready and very important for the future of hypersonic communications. Therefore, for maintaining communications with any hypersonic vehicle or projectile, improvements to the model presented in this thesis and the expansion of this research are very important.

References

1. Gillman E., Blankson I. and Foster J., “Review of Leading Approaches for Mitigating Hypersonic Vehicle Communications Blackout and a Method of Ceramic Particulate Injection Via Cathode Spot Arcs for Blackout Mitigation,” NASA/TM—2010-216220, 2010. URL https://ntrs.nasa.gov/api/citations/20100008938/downloads/20100008938.pdf.

2. Mackey L. and Boyd I., “Analysis of Hypersonic Flow Effects on Sensor Performance,” AIAA Aviation Forum, 2016-4103.

3. Lin, TC, Sproul, L.K., “Influence of reentry turbulent plasma fluctuation on EM wave propagation,”, Computers and Fluids Vol. 35, No. 7, pp. 703-711 (2006).

4. Bird, G., “The DSMC Method,” , 2013.

5. Lu, X., and Ye Z., ”A Universal Method of Redistributing Relaxation Energies in Inelastic Molecular Collisions”, American Institute of Physics, Physics in Fluids, Vol. 34 No. 3, (2022).

6. Siegrist, K., ”The Maxwell Distribution”, LibreText Statistics, April, 2022.

7. Pikus, A., “DSMC/SPARTA Lecture 1,” , 2019. URL https://www.youtube.com/watch?v= cSFr8MTr30Yt=1687s.

8. Schouler, M., Prevereaud, Y., and Mieussens, L., “Survey of Flight and Numerical Data of Hypersonic Rarefied Flows Encountered in Earth Orbit and Atmospheric Reentry,” , Progress in Aerospace Sciences, Vol. 118, 100638, (2020).

9. Brieda, L., “Particle In Cell,” , 2012. URL https://www.particleincell.com/2010/es-pic-method/.

Appendix

Appendix A: Additional Results.

Summary. As flow solvers improve at accurately solving for species number densities in hypersonic flows, the largest obstacle remains the lack of test flight data and the lack of valid wind tunnel data. Since the high surface temperatures are difficult to reproduce in a wind tunnel, and since heat shield nanotubes and vehicle surface materials are very expensive, the phenomena of ablation during hypersonic flight becomes very difficult to gain a robust understanding of. Along with the high strengths, the high melting points of Silicon Nitride and Silicon Carbide make them good candidates for hypersonic vehicles and their sensor windows. In order to begin to understand heat ablation and its effects on hypersonic flow fields and the plasma sheath, one must first look at these materials and how they impact the flow field upon breaking off and then entering the flow. Particles of Silicon Carbide - the vehicle fuselage material, and particles of Silicon Nitride - RF sensor window material - were considered in two simulation cases using Starfish DSMC code [9]. This code is an open-course solver written by Lubos Breida, a professor at USC and founder of Particle In Cell Consulting LLC. The sheared silicon nitride and silicon carbide particles are placed at the center of the flowfield and are approximated as spheres with a diameter of $10\mu m$ for the 2D simulation.

Results. The results of the simulation of the heat ablation using Starfish PIC Solver are shown in Figure 19.

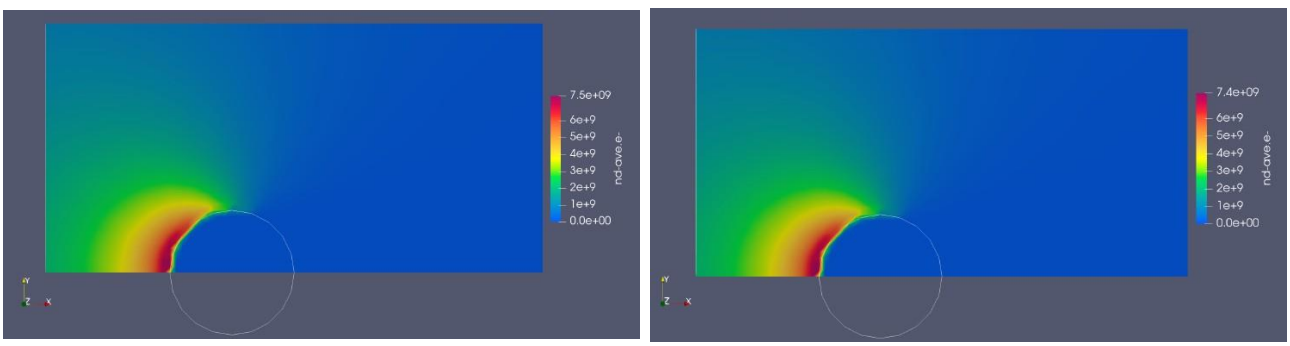

Figure 19 Electron Number Density Profiles around Silicon Carbide (left) and Silicon Nitride (right) Spherical Particles at Mach 5- and 0-degree Angle of Attack

Conclusion. The computational results for Silicon Nitride and Silicon Carbide are very similar, as expected. High speed collisions with free stream gas molecules in front of the particle lead to dissociation and high electron number densities. The maximum number of electron densities are only a fraction of a percent higher than those from the vehicle surface simulation and therefore would not change the results of the BODE plot. In a realistic flow with many surfaces and sensor particles breaking off, it would be necessary to study how RF signals are affected by the accumulation of many high temperature SiN and SiC particles directly in their line of sight. However it does not appear that one individual ablation particle greatly increases the electron number density.